Charles University

Faculty of Science

Study programme: Hydrology and hydrogeology

Adriana Kevešová

UAV MONITORING OF MONTANE PEATBOGS

UAV MONITORING HORSKÝCH RAŠELINIŠŤ

Type of thesis:

Bachelor´s thesis

Supervisor: prof. RNDr. Jakub Langhammer, Ph.D.

Prague, 2022

Zadání bakalářské práce

Název práce: UAV monitoring horských rašelinišť

Cíle práce:

- Vyhodnotit potenciál UAV technologií pro monitoring stavu a změn horských rašelinišť
- Rešerše UAV technologií a metod analýzy obrazu, vhodných pro monitoring rašelinišť
- Pomocí vybraných metod UAV monitoringu, fotogrammetrické rekonstrukce a klasifikace obrazu provést analýzu horského rašeliniště na Rokytce na Šumavě

Jazyk práce: angličtina

Datum zadání: 3.12.2021

Řešitel práce: Adriana Kevešová

Podpis řešitele: .....

Vedoucí práce: prof. RNDr. Jakub Langhammer, Ph.D.

Podpis vedoucího: .....

Prohlášení

Prohlašuji, že jsem tuto závěrečnou práci zpracovala samostatně a že jsem uvedla všechny použité informační zdroje a literaturu. Tato práce ani její podstatná část nebyla předložena k získání jiného nebo stejného akademického titulu.

V Praze dne .....

.....

Adriana Kevešová

To whom it may concern, Thank You.

Contents

Abstract

This thesis deals with UAV imagery analysis as used to monitor environmental settings, in this case a particularly sensitive ecosystem of a peatbog. The non-destructive aspect of UAV monitoring based on remote access to the studied area is crucial in this scenario. Introduction to the topic, examples of the employment of UAV technologies and the possibilities of their application in monitoring peatbogs are followed by examples of visual data analysis with the help of various software on the multispectral data acquired at peatbog Rokytka in the Šumava National Park.

Key words: UAV, monitoring, peatbogs, remote sensing, multispectral imaging, classification

Abstrakt

Tato práce se zabývá analýzou UAV snímků využívaných k monitorování prostředí, v tomto případě zvláště citlivého ekosystému rašeliniště. Za těchto okolností je zásadní nedestruktivní aspekt monitorování UAV plynoucí z dálkového průzkumu studované oblasti. Na úvod do problematiky, příklady využití UAV technologií a možnosti jejich aplikace při monitorování rašelinišť navazují příklady vizuální analýzy dat pomocí různých softwarů na multispektrálních datech získaných na rašeliništi na Rokytce v Národním parku Šumava.

Klíčová slova: UAV, monitoring, rašeliniště, DPZ, multispektrální snímkování, klasifikace

1. Introduction

UAV or Unmanned Aerial Vehicle is a remote sensing platform used to gather spatial information of the observed object or area from a distance. Certain types of UAVs, commonly known as drones, have some autonomy, meaning they can fly themselves according to sensors or are pre-programmed while other UAVs require human intervention. Sometimes referred to as unmanned aerial system (UAS), a term which includes not only the UAV but also sensor payloads (camera), and a ground control system. Various types of sensors or cameras are used, including thermal, multispectral, and hyperspectral cameras or light detection and ranging (LIDAR) systems (Rai et al. 2021). In the acquisition of the data, this thesis works with a multi-rotor UAV teleoperated by a human operator with a remote controller.

There is a certain discrepancy in relation to the definition of UAVs and drones. Although in reality it is not a particularly important matter considering the technological advances the definitions might as well be arbitrary, both terms are widely used interchangeably.

"UAV is an aircraft that can fly without a pilot onboard. UAVs can be either remote controlled that is operated remotely by a human operator from the ground control station or can fly autonomously by an onboard computer." (Rai et al. 2021)

"In recent years, unmanned aerial vehicle (UAVs) or drones have become increasingly useful..." Used as synonyms by Reischig and Cordes (2020)

"[UAV is]an aircraft that is operated from a distance, without a person being present on it. Synonym: drone." (Cambridge English Dictionary 2022)

"UAVs are drones, although not all drones are UAVs." (Ukhurebor et al. 2022)

"*UAS [Unmanned Aerial Systems] are known under various different names and acronyms, such as "Unmanned Aerial Vehicle" (UAV), "aerial robot" or simply "drone," with "UAV" and "drone" being the most popular terms. The term UAS was adopted by the US Department of Defense (DOD) and the Civil Aviation Authority (CAA) of the UK. The International Civil Aviation Organization (ICAO) has introduced the concept of "Remotely-Piloted Aerial System" (RPAS), a particular class of UAS, in the ICAO Circular 328. This term is basically motivated by the fact that only RPAS will be*

able to integrate into the international civil aviation system." From the chapter "On names and acronyms" by Colomina and Molina (2014)

Imagery acquired with the help of a UAV can be used to capture and later analyse various environment indicators and is used in the fields of agriculture or urbanism as well as in the field of environment conservation. While trying to inflict as little as possible additional damage, reliable and detailed quantitative data can be collected. The gathered information can be used to monitor a revitalisation or aid in creating a plan for the revitalisation.

Access to and surveying of peatbog environments is partially restricted, due to which modern monitoring practices that create less of an impact on protected areas are highly valued (Lendzioch et al. 2021). In the Czech Republic, the existing peatbogs are very small areas which cannot be monitored by traditional remote sensing technology such as satellites due to their low spatial resolution, which does not provide sufficient information on the state of peatbogs. A peatbog is not a discrete bounded area. Most areas where peatbogs are found are made up of multiple smaller patches which can be classified as peatbogs but the environment in between them should be also taken into context. This causes variability of the environmental characteristics in the area while still maintaining the continuity of more or less wet soil or organic matter.

While UAV technology is making both monitoring of restored areas and targeting areas for possible revitalisation easier and more effective, traditional surveying methods are still important to verify remotely acquired data by performing an *in-situ* survey (e.g., Clutterbuck et al. 2018, Luscombe et al. 2015).

Peatbogs, a type of peatlands, are water-logged reservoirs with a unique hydrological regime whose typical characteristics include low pH and a high water table. They are places where organic matter is stored, and *Sphagnum* (a peat-forming moss) is an important part of the vegetation composition (Lendzioch et al. 2021). The NRCS Curve Numbers method classifies peat as an impermeable soil of category D (Vlček et al. 2012). While covering approximately 2-3% of the global land surface peatbogs hold 21-25% of the carbon stored in terrestrial ecosystems but this storage is highly vulnerable to ecosystem disturbances (Beyer et al. 2019). Since they are an important soil carbon stock, they will have a major contribution to soil carbon loss over the next century because of climate warming. Additionally, peatbogs are typical for northern ecosystems, which

experience an even faster rate of warming than ecosystems in milder climates. While an increase in frequency and intensity of heavy precipitation was detected, so were drought events, and climate models show that heavy precipitation episodes lead to longer periods of continuous dry days at the expense of lighter and more moderate precipitation. For example, the *Sphagnum* mosses are well adapted to wet conditions, but increasing temperatures and drought stress pose a threat to them (Jassey, Signarbieux 2019). As a result, *Sphagnum* could be replaced by vegetation which is better adapted to these conditions and although it could produce more biomass, its carbon accumulation properties are weaker. A small change in environmental conditions can have a big impact on mires – of which peatbogs are a subtype (Bufková, Křenová, Bastl 2021).

Peatbogs have been transformed by drainage for agricultural needs, forestry, or peat extraction. As a result, their functions, such as nutrient and water retention, water purification and providing a habitat for plants and animals, have been lost. These losses lead to declining biodiversity, greenhouse gas emissions, nutrient leaching, or erosion (Beyer et al. 2019). It is vital to continue restoring peatbogs to their natural state so they can fulfil their functions and not contribute to climate change. As well as before the start of the restoration to recognise the needed measures and after the restoration is completed, to monitor the restoration site for changes and the impact of restoration, UAV monitoring is proposed to be used.

The goal of this thesis is to evaluate the potential of UAV technology in monitoring state and change of montane peatbogs and research methods of imagery analysis which are suitable for this monitoring in the theoretical part of the thesis. Consequently, with the chosen methods of UAV monitoring, photogrammetric reconstruction and image classification to carry out partial analysis of the montane peatbog on the Rokytka stream in the Šumava National Park. The chosen methods were, aside from photogrammetric reconstruction, using supervised classification to determine the land cover and comparing the land cover classes using a spectral index, and some other methods were outlined as well.

2. UAV monitoring

2.1. UAV platform

Applications ranging from fire extinguishing through underground infrastructure maintenance to drone sports show that UAV technology has an especially wide use (Blyenburgh 2022). The RPAS Yearbook, which was being published by Blyenburgh (2021), used to categorise UAV platforms, but has been since discontinued and categorisations used in other publications sometimes vary. For the purposes of this thesis, we will be using the following categorisations based on Radoglou-Grammatikis et al. (2020).

The first classification is based on aerodynamic features and includes fixed-wing, multi-rotor, and hybrid UAVs. Fixed-wing UAVs can be additionally divided into straight-wing, swept-wing, and delta-wing. Among the disadvantages compared to other UAV platforms are the ability to only travel forward and the need for open space for horizontal take-off and landing (Amarasingam et al. 2022). This construction enables the UAV to turn around roll, pitch and yaw angles. Additionally, Seier et al. (2021) note based on their study of disturbances caused by UAVs that it is also likely that the generally quieter fixed-wing UAVs present a milder disturbance on wildlife. Multi-rotor UAVs with three to eight propellers are simple to deploy, flexible and they can fly in all four directions with minimal space requirements for vertical take-off and landing (Amarasingam et al. 2022). The airflow of the multi-rotor UAV is composed of several rotors that generate the power which is necessary for lifting. That is why this type does not need a forward airspeed for lifting. Depending on the number of rotors, a multi-rotor UAV can be classified as a tricopter, quadcopter, hexacopter and octocopter. The hybrid UAV combines the characteristics of the previous ones, namely rotors for take-off and landing as well as fixed wings for covering large areas (Radoglou-Grammatikis et al. 2020). The multi-rotor UAVs are considered better suited where accuracy of the data and a better representation of environmental features is needed as well as for close inspections and where more detailed data on a smaller area is required for enhanced land surveying. Particularly vegetation representation and erosion gully representation were considered (Boon, Drijfhout, Tesfamichael 2017). In another case study the accuracy of the dense point clouds was considered comparable, but the advantage of the multi-rotor UAV with higher redundancy in collected data was in the lower processing time, higher point density and lesser data gaps (Gonçalves et al. 2021).

There is a certain degree of autonomy to each UAV although there is a big difference between an automatic UAV which has been programmed for a very specific task and an autonomous UAV which obeys rules that adjust its behaviour and either has the ability to perform some decisions under human supervision or is fully autonomous. UAV can also be a part of a fully human-operated system (Radoglou-Grammatikis et al. 2020).

Another categorisation can be based on the type of power source being kerosene, battery cells, fuel cells or solar cells. Large fixed-wing UAV used for military purposes is the type usually powered by kerosene. The small rotary-wing UAVs use battery cells because they are equipped for less operating time. A fuel cell, an electric device which transforms chemicals into electrical energy, can only be incorporated into fixed-wing UAVs and it is used for maximising the flight distance, making fixed-wing UAVs favourable where there is a need for longer battery life (Radoglou-Grammatikis et al. 2020). UAVs can be also categorised based on their maximum gross take-off weight, normal operating altitude, or airspeed (Yao, Qin, Chen 2019).

2.1.1 UAV sensors

An important part of the payload of UAV are sensors, a camera being the most used one. The three main types of cameras are multispectral, hyperspectral, and thermal.

Another illustration of variable terminology and categorisation is that Yao et al. (2019) state that multispectral cameras can contain up to a few tenths of bands in addition to RGB bands, Radoglou-Grammatikis et al. (2020) state that multispectral cameras "*integrate five bands"* and Nex et al. (2022) state that multispectral cameras can have up to 10 bands and simultaneously that RGB cameras belong to the category of multispectral cameras. Nonetheless, these bands are optimized on specific spectral regions with the most common ones being blue, green, red, red-edge and near-infrared. Among the emerging applications for multispectral sensors are leaf level disease assessment or harmful algae bloom studies (Yao, Qin, Chen 2019).

Hyperspectral cameras provide contiguous spectral signatures by obtaining tens to hundreds narrow spectral bands. Hyperspectral cameras are currently still used mainly for scientific or research purposes as they are quite expensive, heavy, and more challenging to operate compared to optimised multispectral cameras. They capture vast volumes of data whose analysis can be more demanding (Nex et al. 2022).

2.2. Photogrammetric reconstruction

The technology of aerial photogrammetry involves obtaining reliable information about objects or the whole environment in three dimensions, primarily in the visible light spectrum and can also be used in the near-infrared spectrum. This technology is widely used in the natural resource management and other natural sciences. With the help of techniques such as geometry, trigonometry, or optics, it is a method to identify the properties of studied objects (Bettinger et al. 2017). Fundamentally triangulation is used to mathematically intersect lines of sight, which connect the camera to points on the object on photographs taken from multiple different locations. This way, the three-dimensional coordinates of the points of interest are created. It is the same principle on which human eyes work when determining distance. This is called the depth perception (Horswell 2013). Overlapping vertical aerial photographs are required to create an analytical model which can compute the coordinates of features using photogrammetry techniques. A georeferenced digital orthophotograph can be developed by combining the overlapping vertical aerial photographs, removing topographic displacement or other distortions analytically and georeferencing them (Bettinger et al. 2017). Photogrammetric reconstruction of UAV data can produce 2D output, similar to more traditional remote sensing solutions such as using satellite data, as well as a 3D output which also has a high resolution, capturing detail down to lower centimetres.

2.2.1 Structure from Motion

Structure from Motion (SfM) as a method of photogrammetric reconstruction uses, similarly to traditional photogrammetry, overlapping images acquired from multiple positions. The three main advantages SfM has over traditional photogrammetry are as follows. Firstly, the features are automatically identified and matched in images of different scales, viewing angles and even light conditions. Secondly, the equations used in the algorithm can be solved without information about camera position or ground control points. Lastly, the camera calibration can be automatically refined during the process (Iglhaut et al. 2019).

There is a range of SfM tools available for PCs and there are also web-based apps which provide similar services for 3D model generation. The first type of solutions processes data on the local machine, an example being Agisoft PhotoScan and the second type uploads images to a server where it is processed and the result can be downloaded, this is how, for example, Microsoft Photosynth works. Most SfM platforms are automated

allowing the generation of 3D data which does not require increased user supervision and expertise. There are even low-cost processing systems available online which allow the processing to be done in a few minutes, for example already during field data collection. The exact implementations of the SfM algorithm may vary. In fact, these platforms provide a black-box tool and might cause the user to not be able to control the data quality and the errors in data might end up overlooked. For example, the fully automated software packages do not assume that the same camera was used to capture all of the imagery and each frame can be calibrated individually. Inappropriate image overlaps can generate inaccurate camera models and consequently inaccurate datasets (Micheletti, Chandler, Lane 2015).

Concerning the SfM workflow (Fig. 1), first, an automatic extraction of keypoints is carried out. Keypoints stand for points which have distinctive contrast or texture, they are matched across images where they appear. For the keypoints to be accurate, a visually distinct texture must appear in the imagery which can prove to be a problem with certain environments or lighting conditions (Micheletti, Chandler, Lane 2015). This keypoint matching is carried out by the scale-invariant feature transform (SIFT) algorithm and works on the basis of assigning numerical descriptors which are invariant to scale and orientation to each point in each image. Thus, the coarse geometry of the location can be reconstructed and used to check the coherence of keypoint matches. With the help of a sufficient number of keypoints and images, bundle adjustments can be performed, and camera parameters can be computed. A sparse point cloud consisting of keypoints is the output of the process (Iglhaut et al. 2019). Initialization values obtained from sequences of randomly selected matched keypoints and parameters from the cameras are used to solve the bundle adjustment, which is the joint non-linear refinement of point parameters and camera parameters that minimizes the reprojection error using a function that projects scene points to image space and a function that can potentially down-weigh outliers (Schonberger, Frahm 2016). Dense image matching algorithms such as Multi View Stereo (MVS) are used subsequently to SfM algorithm in order to make the point cloud denser (Iglhaut et al. 2019). As MVS is understood a group of techniques, which use stereo correspondence as their main resource and use more than two images (Furukawa, Hernández 2015). Additional processing steps usually involve the derivation of a digital surface model (DSM) and an orthomosaic.

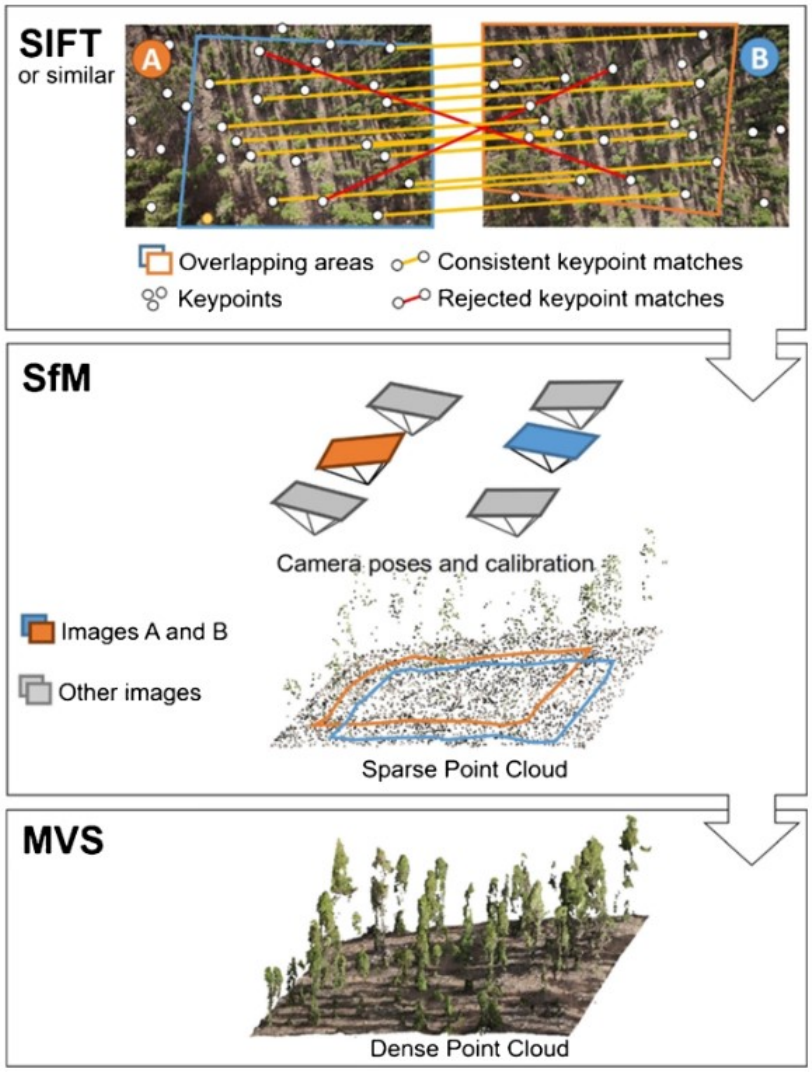

Figure 1: SfM workflow (Iglhaut et al. 2019)

The results of photogrammetry are highly influenced by the imagery on input. Because of this, the types of sensors and their settings should be carefully inspected, and lightning conditions should be taken into consideration as well. As far as the choice of a sensor goes, a camera equipped with a fixed focus lens has to be used. Images are not required to be taken from the same distance or to have the same scale. Quite the contrary, it is advised to capture the site in multiple scales, initially obtaining imagery of the whole site with a few frames before capturing smaller range images. It is also critical to acquire the highest possible amount of imagery from different positions. The wide range of images taken from different directions then creates a dataset with an accurate geometry, which is important in recovering both internal camera models and object coordinates (Micheletti, Chandler, Lane 2015). It is recommended for the longitudinal and transversal overlap to be at least 80% and 60%, respectively (Nex, Remondino 2014).

2.3. UAV data analysis

Land cover mapping is one of the typical outputs of RGB imagery analysis. Pixel-based classification is used on satellite RS data but is not as suitable for UAV data as the inter-pixel similarity and inter-pixel variance are both very high. Object-based analysis is required and an additional need for combining 3D information, like height and geometric information, arises. Additional contextual information and deep learning methods improve accuracy (Yao, Qin, Chen 2019). For advanced vegetation analysis, red-edge and near-infrared bands are used in types of spectral indices, the vegetation indices (see 2.3.1). Thermal imaging was first used in military context but is nowadays common for applications like forest fire monitoring (Colomina and Molina 2014).

2.3.1. Spectral indices

Vegetation indices are mathematical transformations created for evaluating the spectral contribution of vegetation to multispectral observations (Elvidge, Chen 1995). While some vegetation indices can be derived from RGB sensors, such as the normalized greenness indices, their spectral sensitivity to the chlorophyll level of the vegetation required, e.g., for plant health evaluation or disease diagnosis, is not sufficient. Near-infrared cameras are required to calculate vegetation indices like Normalized Difference Vegetation Index (NDVI), Green Normalized Difference Vegetation Index (GNDVI) or Enhanced Normalized Difference Vegetation Index (ENDVI) (Yao, Qin, Chen 2019). Chlorophyll pigment absorptions in the red spectrum are contrasted against the high reflectivity of vegetation in the near-infrared or red-edge spectres and indices can be used to analyse processes such as vegetation productivity and evapotranspiration (Elvidge, Chen 1995).

A reflectance calibration is of prime importance before the calculation of vegetation indices. This is done by capturing images of a reflectance panel in all used bands in such conditions that it is not covered by any shadows and is set to be as horizontal as possible (Raeva, Šedina, Dlesk 2019).

The NDVI was first developed for use with LANDSAT imagery, and it quantifies the amount of living vegetation in a pixel. Green leaves absorb visible light from 600 to 700 nm and reflect near-infrared light from 700 to 1100 nm so in case that there is a lot more reflected radiation in near-infrared wavelengths than in visible light wavelengths, the vegetation is likely to be green. The equation for the calculation of the NDVI is:

$$NDVI = \frac{NIR - R}{NIR + R}$$

Where R stands for the average signal intensity in the wavelength range of the visible red light and NIR stands for the average signal intensity in the wavelength range of near-infrared radiation. The NDVI for a given pixel is equal to a number in the range from -1 to +1. While a negative value corresponds to water, values close to zero mean no vegetation like in the areas of rock or snow and a value near one indicates the highest possible density of green leaves. (Arnold et al. 2013).

GNDVI is similar to NDVI, but it uses the green light instead of the red one, which makes it more sensitive to chlorophyll. The equation for the calculation of the GNDVI is:

$$GNDVI = \frac{NIR - G}{NIR + G}$$

Where G stands for the average signal intensity in the wavelength range of the green visible light. The values of GNDVI fall into the range of [−1, + 1] and they are usually higher than the NDVI values as the wavelengths in the green part of the spectrum are shorter than the red ones (Raeva, Šedina, Dlesk 2019).

With some sensors also Normalized Difference Red Edge (NDRE) index can be used, and it indicates the rapid change in vegetation reflectance between the visible red and near-infrared light. NDRE is sensitive to chlorophyll content in plants' leaves, variability in leaf area as well as background effects. The equation for the calculation of the NDRE is:

$$NDRE = \frac{NIR - RE}{NIR + RE}$$

Where RE stands for the average signal intensity in the wavelength range of the red-edge radiation. The NDRE values range between −1 and + 1, while the higher the values, the higher the amount of chlorophyll. It is claimed that the NDRE is a better indicator of plant health than the NDVI for vegetation with a high level of chlorophyll (Raeva, Šedina, Dlesk 2019).

2.4. UAV monitoring of peatbogs

UAV technology is used for monitoring peatbogs on the one hand for the same reasons as any other environment which is that it offers the opportunity to assess large spatial extents in less time than traditional methods do but on the other hand the peatbog vegetation is often sensitive to trampling and UAVs present a non-intrusive method for ecological monitoring (Clutterbuck et al. 2018). There have been studies on videographic analysis of vegetation coverage (Kalacska et al. 2013), an object-based classification of restored bog surface (Knoth et al. 2013) or another object-based classification done in order to study CH_4 fluxes (Lehmann et al. 2016) and also a mapping of the groundwater table (Lendzioch et al. 2021). Following are examples of partial analyses which are being carried out on peatbogs or in similar environments with possible applications on a peatbog.

2.4.1 Water surface extent

The literature on determining the water surface extent on a local scale is scarce, more often satellites are used to determine water surface on a larger scale (e.g., Musa et al. 2015). According to Tymków et al. (2019) it is possible to determine water surface extent at a local scale with only 2D data, there's no need for 3D data which would come with the need for a more complex analysis. Data from RGB cameras is usually used, but the results proved to have better accuracy with the addition of a thermal infrared (TIR) band. Water covered with vegetation, such as duckweed (*Lemnoideae*), seems to be problematic when identifying the proper extent of surface. This is the case for stagnant water, identifying the extent of surface for flowing water bodies is more credible, in case of a peatbog some of the water is stagnant and can be covered by various vegetation or algae which would not seem to be the same category as clear water in most classifications.

Another problematic aspect of determining the water surface borders is the fact that the waterside is often occluded by higher vegetation (when using 2D data). This can be avoided by using active remote sensing, precisely LiDAR, to create a point cloud where the points of laser reflection of vegetation can be filtered out while leaving the points of the laser reflection of the ground because some laser rays will be able to pass through the leaves (Tymków et al. 2019).

2.4.2 Exploitation, modification, and revitalisation monitoring

The use of UAVs for revitalisation of restoration monitoring is encouraged as a technology which is reliable and cost-effective particularly in restoration sites of small extent where satellite data are not applicable as they do not have the required spatial resolution because these areas are often made up of a fine-scale mosaic of different habitat patches. A possibly higher temporal resolution might be an asset in the case of a dynamic site with frequent disturbances even within hours or days. It is shown that enough important parameters can be obtained from standard RGB images captured by an UAV and processed with GIS (Woellner and Wagner 2019).

There is also a problematic aspect of using UAS for monitoring in protected areas. Out of the investigated studies, 77% of those deemed relevant for the management of protected areas did not discuss or even mention any potential impacts caused by UAS which is regarded as reflecting a low awareness of UAS users for possible disturbances. It is concluded that the possibility of disturbance is not sufficiently considered, and it is stressed for protected area managers and study designers to take actions concerning controversial use of UAS and to have mitigation measures in mind. The actual impacts reported included mostly minor disturbances, but some studies proved the behavioural impact on nesting waterfowl and other species of birds. The options to reduce the impact of the devices on wildlife were studied and some of the proposed measures include not flying trajectories which follow a species' movement pattern, flying at a fixed height and only using an UAS when it is justified by a scientific monitoring concept, particularly in protected areas which are parts of national parks (Seier et al. 2021).

In Šumava National Park, where the study area this thesis deals with is located, the already existing artificial drains are being covered with soil or the water flow in them is slowed down by structures not only around the Rokytka peatbog. The project Life for mires (Life 2019), aside from other activities, organises events for volunteers working towards revitalisation of peatbogs, for example by helping to cover the artificial drains. A work in progress of removing one of these drains and creating pools for water detention separated by wooden beams can be seen in the south-western corner of the study area (see digital appendix – orthophoto of the whole area). Restoration measures such as wooden dams (Fig. 2) are aimed at decreasing fluctuation and increasing groundwater level (Doležal et al. 2017). Such measures could be monitored by UAV technology in terms of evaluating moisture characteristics (see 2.4.4).

Figure 2: A wooden dam in Šumava National Park Photo: A. Kevešová, 2022

There is a UAV-based method developed using near-infrared spectrum for supporting restoration monitoring of cut-over bogs. It provides information on species distribution and the surface structure with a two-step classification process of automatic image segmentation and object-based classification. These are used to distinguish between multiple pre-defined classes of waterlogged bare peat and various vegetation. An independent validation procedure has showed a high accuracy of this classification. These cut-over bogs can be a source of carbon instead of being a sink for it and vegetation characteristics of restored peatbogs can be used as indicators to assess the state of the peatland concerning carbon sequestration (Knoth et al. 2013).

2.4.3 Peatbog vegetation evaluation

Traditional biodiversity monitoring includes invasive and/or costly methods such as ground sampling, the use of manned aircraft or satellite imagery to get information about the area of interest. Lately UAVs are used more often to monitor vegetation and while being already the cheaper option, they offer a better spatial and temporal resolution and the data deployment is faster, which makes it a fast-evolving technology in this field (Lehmann et al. 2017).

There have been attempts at creating a neural network which is trained to identify various types of vegetation (e.g., Zhang et al. 2020, Kattenborn et al. 2020). An overview of the use of convolutional neural networks shows applications in the fields of forestry, agriculture, or conservation. The utilized advanced neural networks must be edited based on the exact task they are used for, and reliable training data must be provided as well (Kattenborn et al. 2021), which in case of vegetation identification would mean a more detailed survey of at least part of the study area would need to be carried out on the basis of which individual plants could be identified.

Deep learning is also used for supervised classification of land cover with the use of various algorithms such as Support Vector Machine (SVM) or Random Forest (RF) classifiers (Catalyst 2022). Simple classifiers like these or maximum likelihood classifiers might prove to not be sufficient as the scene contents get more complex. An ensemble of simpler classifiers or deep learning based methods, belonging among more advanced methods, still present a huge potential, which is being explored for the ultra-high-resolution, multi-modal data (including height, thermal, and hyperspectral information) which can be acquired with the use of UAV (Yao, Qin, Chen 2019).

Another possibility of identifying vegetation is generating a 3D surface model using structure-from-motion methods. This way, it is possible to detect the vegetation height and thus identify spectrally similar vegetation with different height (Beyer et al. 2019).

2.4.4 Evaluation of temperature and moisture characteristics

Thermal imagery was used to measure near surface wetness in an upland peatland catchment. Simultaneously, an airborne LiDAR sensor was used to support the results of the analysis of thermal imagery. It was found that areas of higher relative thermal emissivity (ε_r) are located in topographic sinks and along surface flow networks and lower, where anthropogenic drainage systems are still functional. It is suggested that this and other findings, such as the type of vegetation found in the different locations, imply that areas with higher ε_r may be wetter. However, authors of this research admit this isn't generally true as they have recorded that high surface structure (e.g., trees) has a strong control over the ε_r value and, on the contrary, some variations in ε_r were found to be independent of any drainage features. The effect of surface structure on ε_r was mitigated by taking the LiDAR data into consideration, reducing the influence of vegetation, and creating a relative ε_r. Field survey was also used to validate the spatial association

between ε_r and measured surface wetness. This relationship is observed due to relatively high specific heat capacity (C) of water (4.1855 J g K^{-1} at 15 °C, 101.325 kPa) and the fact that the ability to resist heat loss is higher for water than for other surrounding landscape components (Luscombe et al. 2015).

2.4.5 3D models of peatbog

In addition to the visual identification of individual plants with UAV imagery, natural erosion features as well as artificial drainage appear very well-defined. Artificial drains and drainage gullies in degraded peatland areas are associated with erosion and lowering of water tables, which can promote decomposition of peat. It can also have an impact on water quality and on the composition of nearby vegetation, including the important peat forming species. These features can be identified so clearly that it is likely that the digital surface model (DSM) derived using UAV data is going to become a strategic tool for monitoring peatland erosion (Fig. 3). A fixed wing UAV was used to survey a blanket mire complex, Howden Moors, from a height of 60 m above the ground. Two flights were utilized to collect colour (RGB) imagery and near-infrared data independently (Clutterbuck et al. 2018). In Figure 4, a peatbog in the Šumava National Park can be seen where one of the artificial drains has been already revitalised (upper part of the image), and the other has not (lower part of the image).

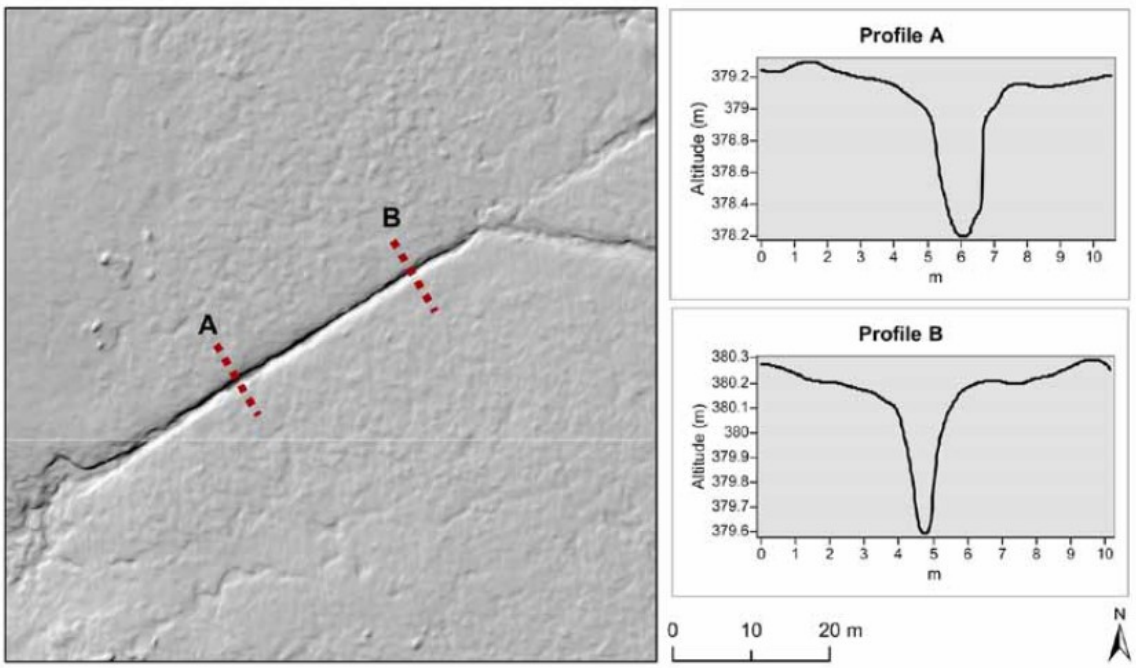

Artificial drain as visible in 0.028 m resolution DSM derived from UAV imagery for Howden Moor and cross-sectional profiles at two locations (note exaggeration in vertical scale).

Figure 3: Artificial drain on DSM (Clutterbuck et al. 2018)

Figure 4: A digital model of relief of part of the Rokytka Moors (ČÚZK no date)

3. Data

3.1 Study area

3.1.1 Šumava National Park

The Šumava National Park is a national park in the South Bohemian regions of the Czech Republic along the border with Germany and Austria. The local climate has a transitional character influenced by oceanic and continental climate. Total amount of precipitation increases with increasing altitude, while the highest amount is reached in the central part of Šumava (Březník 1486–1552 mm in a thirty-year average). The retention capacity of soils in Šumava ranges from 60 to 90 mm (Vlček et al. 2012). The most extensive peat bog complex in Central Europe is located in the Šumava Mountains as a result of the specific geology and morphology of this area. Upland peat bogs like the ones in Šumava Mountains occur in Canada, Scotland, and Scandinavia (Lendzioch et al. 2021).

There were changes occurring in the Šumava Mountains caused by the effort to drain and dry peatbogs as they were traditionally subject to peat and wood exploitation or agricultural land cultivation. The extent to which this was happening was considerable already at the beginning of the 20th century, but the main period of drainage digging was in the 70s and 80s. To this day, the drainage systems are still visible, and it has been proven that drainage has affected almost 70% of peatbogs in the Šumava Mountains. Fast surface flow and higher fluctuation of groundwater level are both caused by these systems of drains. Restorations can improve these problems and at the same time increase the groundwater level by several centimetres in a year (Doležal et al. 2017).

A considerable increase in air temperature has been recorded in the area of Šumava National Park, with both summer and winter temperatures increasing. Ombrotrophic bogs and minerotrophic fens were studied to show the difference of response to the changes in temperature and precipitation while it was concluded that bogs are more vulnerable to these changes as the loss of water through evapotranspiration and reduced precipitation can be compensated by groundwater in case of fens, which is not possible for bogs because of their ombrotrophic nature. Significant reduction of vegetation was observed on studied bogs, especially with species poorly adapted to dry conditions such as *Carex limosa* and *Warnstorfia fluitans* (Bufková, Křenová, Bastl 2021).

There are restrictions in the Czech Republic concerning flying a drone/UAV in national parks and protected landscape areas. According to regulations issued by the Civil Aviation Authority (CAA) of the Czech Republic (2020) the use of UAV in all protected areas but the fourth zone of protected landscape areas is prohibited without a permission of the authority and even there it is only allowed under the condition of not disturbing the protected species. More limitations concern the time of the flight across the year because of the protection of the bird species *Tetrao urogallus*. Apart from restrictions for UAVs there are also restrictions for planes flying above Šumava National Park which can only do so with a permission from CAA and the minimal height of flight must be 300 metres over the highest obstacle in the circuit of 600 metres around the plane (Air Navigation Services of the Czech Republic n.d.).

3.1.2 Peatbog Rokytka

The data used for this thesis were acquired around Rokytka stream, which is located in the central part of the Šumava Mountains and in the area of the Šumava National Park. The studied peatbog is part of a bigger complex of peatbogs called the Rokytka Moors. They are located on moderate slopes near the bottom of the Rokytka stream valley in the Vydra headwaters. Rokytka is a left tributary of Roklanský brook in the basin of upper Otava. Roklanský brook and Modravský brook are the main source of Vydra, which later creates Otava on confluence with Křemelná. From a geological point of view, according to tectonic zoning, this basin belongs to the area of the Vltava-Danube elevation (Moldanubicum) (Vlček et al. 2012). Soil cover in this region composes of entic Podzol, sometimes Rankers in steeper slope areas. The catchment of Rokytka is mostly covered by Histosols while peaty Gley can be found in some parts of the stream floodplains. Total area of organic soils in the whole catchment is at 23% of its surface (Doležal et al. 2017).

The average gradient of slope is only 4°, not very often the gradient reaches 10° while the maximum is 12°. There are a few large and a higher number of small montane peatbogs in this area of almost 250 ha, the depth of the larger peatbogs can reach up to 7 meters (Doležal et al. 2017). The altitude varies between 1089 and 1224 m a.s.l. with the average of 11225 m a.s.l., the basin is quite flat considering its montane location (Vlček et al. 2012).

Specific morphology of the peat bog and the open space area cause the Rokytka catchment to be one of the coldest places in the country throughout the winter. There are

freezing temperatures occurring even during the summer, and the average daily air temperature is 4.8 ◦C. Aside from that, this location belongs to one of the Czech Republic's wettest parts, with humidity varying more during the day than during a year (Lendzioch et al. 2021).

Vegetation in the Rokytka catchment comes from a relict plant community. Mainly low grass with the growth of *Trichophorum caespitosum*, which blends in a mosaic pattern with the hydrophilic vegetation of shallow depressions and the edges of lakes, can be found. Hydrophilic vegetation consists of a mat of *Sphagnum cuspidatum* and *Sphagnum majus* with the growth of the above-mentioned *Carex limosa* and *Scheuchzeria palustris*. Reddish types of peat such as *Sphagnum magellanicum*, *Sphagnum russowii* or *Sphagnum rubellum* can also be found (Doležal et al. 2017). Further to the borders of the peatbog *Pinus pseudopumilio* or *Betula nana* grow, spruce can grow on the borders of the peatbog or near the drainage ditches. The remaining forest vegetation consists mainly of spruce forest with a mixture of fir and beech, which is found especially on the southern slopes. Roughly one quarter of the forest is affected by bark beetles. There are both "dead forests" and clearings partially overgrown with young plants. The herb layer consists of various species of grasses and mosses, and blueberries. A healthy forest has a developed herb and shrub layer and new vegetation, mainly spruce sprouts, seedlings, and grasses, in the "dead forest" is starting to grow again thanks to the wood mass, which was left there (Vlček et al. 2012).

JTSK/Krovak East North coordinates of the centre of the study area are -831501.83, -1149798.75 and the surface is approximately 10 ha.

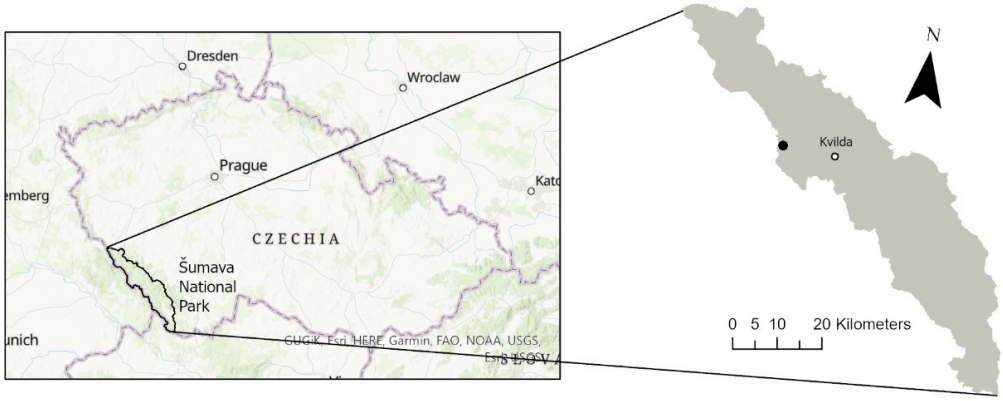

Figure 5: Study area location

3.2 UAV data

Multispectral data was acquired on the 12th of November 2021 with a MicaSense Altum-PT sensor with 5 spectral bands and a thermal band (Table 1, Fig. 6). The raw data was in the form of TIFF imagery with localisation. A control reflectance panel was used to calibrate the imagery because of varying light conditions, while the advantage of using this sensor is the option to only use one reflectance panel. TIFF imagery was geolocated in the WGS 1984 coordinate system (EPSG 4326).

Table 1: Altum PT sensor bands (MicaSense 2021)

Spectral bands	**Blue**	**475 nm center, 32 nm bandwidth**
	Green	560 nm center, 27 nm bandwidth
	Red	668 nm center, 14 nm bandwidth
	Red Edge	717 nm center, 12 nm bandwidth
	Near-IR	842 nm center, 57 nm bandwidth
Thermal	FLIR LWIR thermal infrared	7.5-13.5 µm radiometrically calibrated

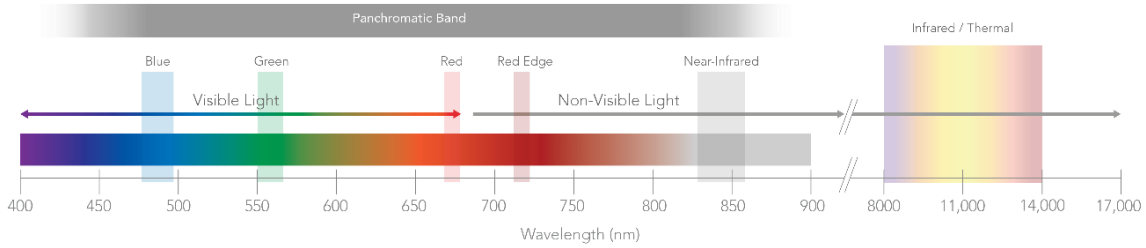

Figure 6: Illustration of the wavelengths of the bands (MicaSense 2021)

4. Methods

4.1. Imagery analysis

4.1.1 Photogrammetric processing

Initial data processing was done in Agisoft Metashape Professional version 1.8.3. It is a photogrammetric processing software which generates 3D spatial data used particularly for processing UAV data. It uses the Structure from Motion technology for photogrammetric reconstruction.

After the data was added, 876 photos were separated into 146 cameras (Fig. 7) and reflectance was calibrated (Fig. 8) using photos of a reflectance panel in each band, which were automatically found from among other photos. Photos were aligned and a digital elevation model (DEM) was created from 42511 tie points. The flying altitude was 87.4 m, the ground resolution is 3.84 cm/pix and the coverage area 0.0981 km^2. Camera properties can be seen in Table 2.

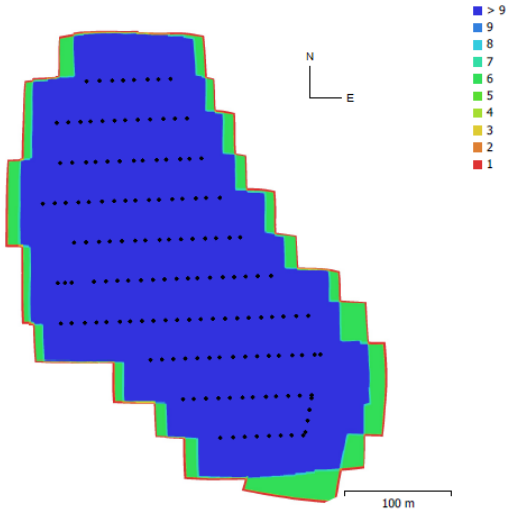

Figure 7: Camera locations and image overlap

Panel Calibration

	Band	Reflectance
1	Blue	0.544
2	Green	0.543
3	Red	0.542
4	Red edge	0.542
5	NIR	0.541
6	LWIR	

Figure 8: Reflectance Calibration Panel

Lastly, an orthomosaic was generated from the DEM. A mesh can also be created, which corresponds to a 3D model.

Table 2: Camera properties

Camera model	Resolution	Focal length	Pixel size
Altum, Blue	2064 x 1544	8 mm	3.45 x 3.45 µm
Altum, Green	2064 x 1544	8 mm	3.45 x 3.45 µm
Altum, Red	2064 x 1544	8 mm	3.45 x 3.45 µm
Altum, Red edge	2064 x 1544	8 mm	3.45 x 3.45 µm
Altum, NIR	2064 x 1544	8 mm	3.45 x 3.45 µm
Altum, LWIR	160 x 120	1.77 mm	12 x 12 µm

4.1.2 Classification

Having generated the orthomosaic in Agisoft Metashape it was imported into PCIDSK format to upload it into Catalyst Professional for imagery analysis. More empty channels to use for processing were added to the file through OrthoEngine and vegetation indices from 2.3.3 were calculated in EASI Modeling with the respective equations (e.g., %8 = (%5-%3) / (%5+%3) for NDVI, where '%8' stands for the first empty channel, '%5' stands for NIR channel and '%3' for the red channel). A bitmap created by the THR algorithm, which thresholds an image to a bitmap, excluding the orthomosaic's background, was created to be used as a mask.

Supervised classification with the Maximum Likelihood algorithm, a foreground mask, without a NULL class and utilizing all captured bands was used to create a land cover map with 5 classes (Fig. 9). Similar classification could be achieved using ArcGIS' Train deep learning model tool or custom code in Google Earth Engine.

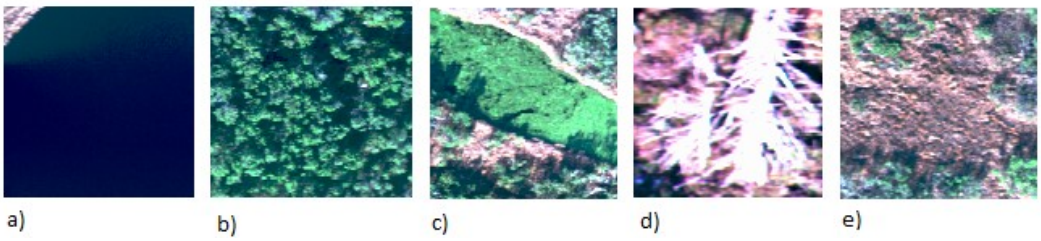

Figure 9: Classes a) water b) trees c) overgrown water d) dead wood e) soil/mud/low darker vegetation

Aside from more advanced methods of water surface detection, simple thresholding can be used on the water surface which is not overgrown with vegetation and thus has very low emission in the near-infrared spectrum. Depending on the objective of this detection, this method can be sufficient for finding clear water surface.

5. Results

The output of the supervised classification is shown, the distribution of NDVI values and the results of the thermal analysis are presented in the chapter Results. Additional analyses are outlined in the chapter Discussion.

5.1 Classification

Classification was generated for five chosen classes, the following tables show the classification characteristics, the confusion matrix, and the accuracy.

Table 3: Supervised classification characteristics

ID	Value	Name	Color	Threshold	Bias
1	1	water		0.50	1.20
2	2	trees		0.50	1.00
3	3	overgrown water		0.50	0.80
4	4	dead wood		0.50	0.01
5	5	soil/mud/low darker vegetation		0.50	1.00

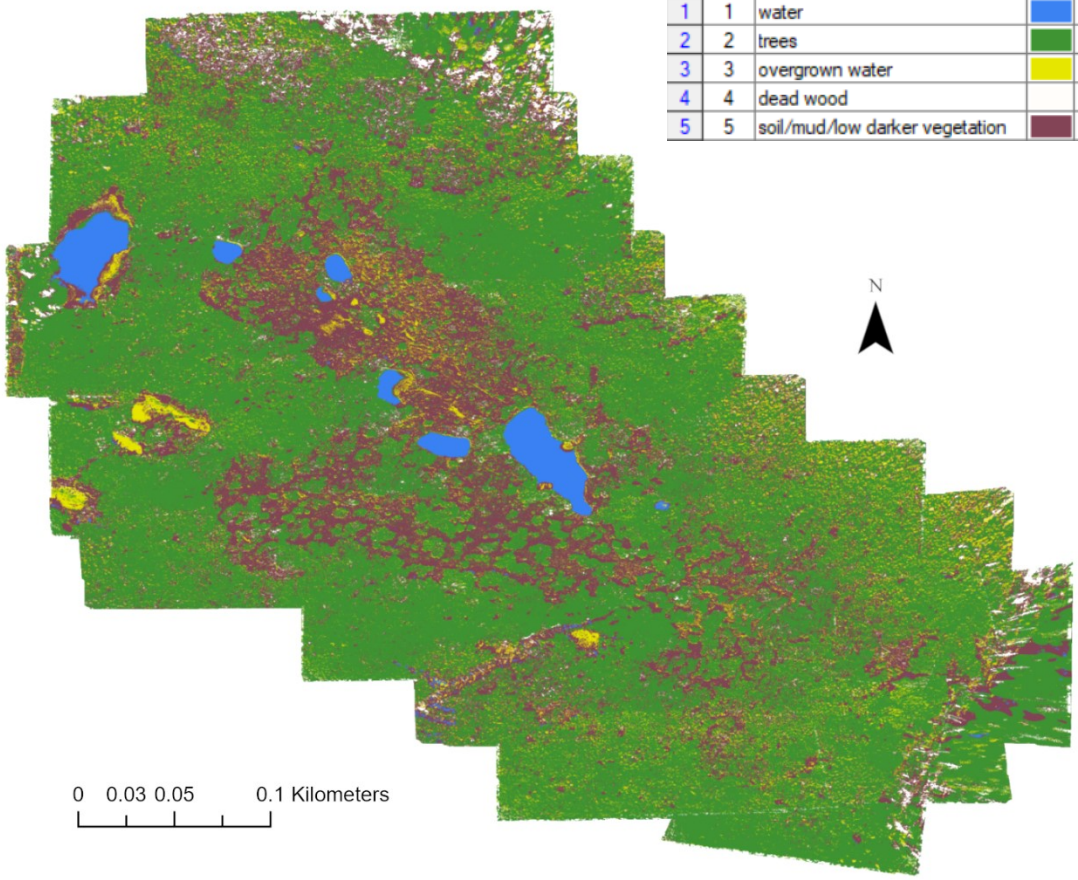

Figure 10: Supervised classification result

Table 4: Supervised classification result

Class	Pixels	
Water	1378062	2.04%
Trees	41749678	61.77%
Overgrown water	5082129	7.52%
Dead wood	2033547	3.01%
Soil/mud/low darker vegetation	17340891	25.66%
Total	67584307	100.00%

Table 5: Confusion matrix

	Pixels	**Water [%]**	**Trees [%]**	**Overgrown water [%]**	**Dead wood [%]**	**Soil/mud/low darker vegetation [%]**
Water	797288	99.19	0.02	0.04	0.00	0.75
Trees	2206811	0.00	92.69	3.62	0.17	3.52
Overgrown water	116665	0.13	6.09	79.36	0.46	13.96
Dead wood	35137	0.00	0.26	1.86	87.51	10.37
Soil/mud/low darker vegetation	217781	0.02	5.09	4.57	0.78	89.55

Table 6: Accuracy

Average accuracy	89.66%
Overall accuracy	93.51%

Bias for the *dead trees* class was lowered substantially for the classification to show a more precise shape of the dead trees and also to not contain pixels which should in fact belong to a different class and are just overexposed. This effect was, however, not eliminated completely. The algorithm identified the *overgrown water* class quite precisely for how variable it is, and it correctly identified small ponds overgrown with algae in the area with bigger lakes in the middle of the map. Though there is a tendency to assign individual pixels to this class and there was an effort to remove it by adjusting parameters but that affected the recognition of said small ponds.

It was found that it may be more effective to choose a smaller training area but with as many characteristics typical for the class as possible than to also include border cases

such as area in shade or area with too many overexposed pixels. In some classification trials, there was a problem with the algorithm classifying shades as either *overgrown water* or *dead wood*. Part of the problem was solved by adjusting bias and part by simplifying the training area.

As the soil pH decreases towards the peatbog the vegetation changes from spruce trees through dried out spruce trees to the shorter conifer *Pinus mungo* which can survive in more acidic soil (Fig. 11). This tendency can be observed in parts of the orthophoto; however, it is not distinguishable enough for the classification.

Figure 11: Vegetation on the edge of the Rokytka Moors, view from inside the area of the peatbog Photo: A. Kevešová, 2022

5.2 NDVI distribution

The number of pixels in the *water* class which have the NDVI value of -1 is 442748, that is 32.1% of all pixels in the class. Pixel has the value of -1 when the signal intensity in the wavelength range of near-infrared radiation is zero, which is typical for water surfaces. Here, a histogram with an edited y-axis can be seen in order for the counts of pixels of different values to be visible.

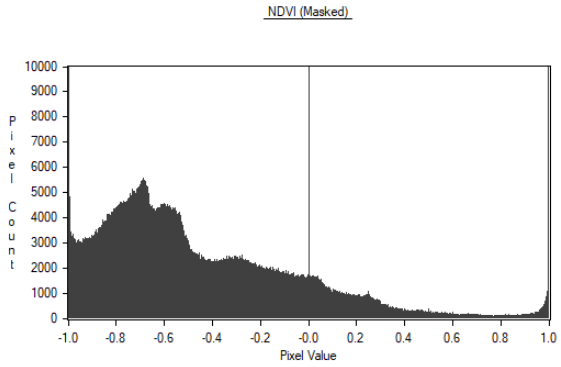

Figure 12: Water class NDVI values

The difference in scale in subsequent histograms should be noted.

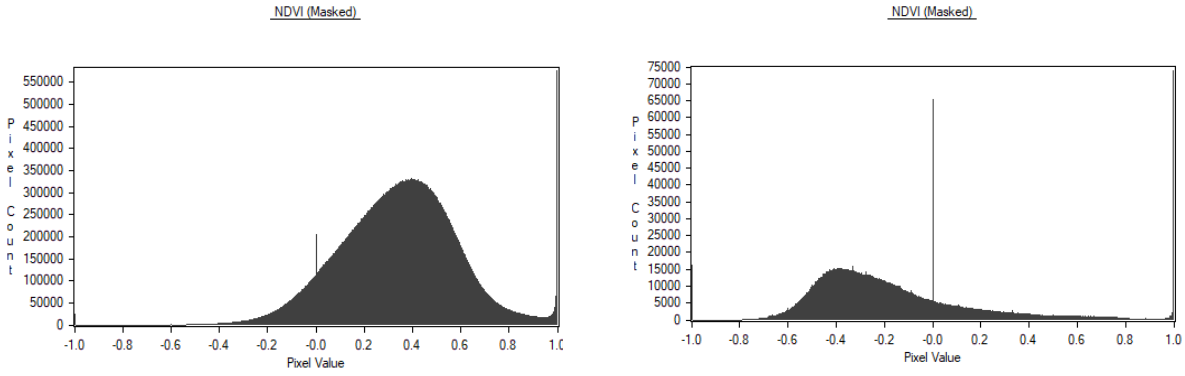

a) trees

b) dead wood

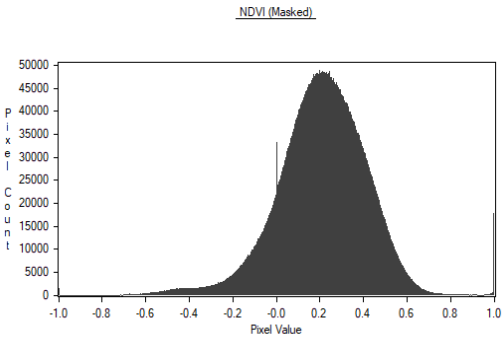

c) overgrown water

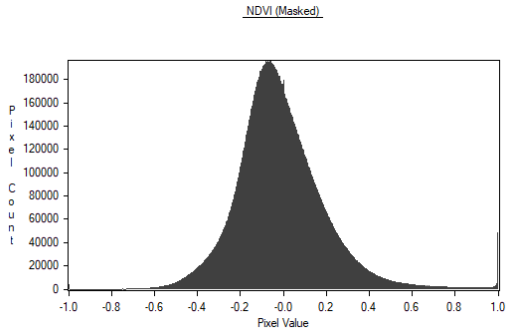

d) soil/mud/low darker vegetation

Figure 13: Histograms of NDVI values of classes

581185 pixels of the class *trees* (Fig. 13a) are equal to 1, which is 1.4% of the total pixels assigned to this class. 75103 pixels of the class *dead wood* (Fig. 13b) are equal to 1, which is 3.7% of total class pixels. Median of 0.22, mean of almost the same value of 0.21 and standard deviation of 0.21 characterise the class *overgrown water* (Fig. 13c). Median of -0.03, mean of a similar value of -0.01 and standard deviation of 0.21 characterise the class *soil/mud/low darker vegetation* (Fig. 13d). In all histograms a spike

in pixel count of the pixel value of 1 can be seen. This happens when there is no signal received in the red spectrum.

Thresholding based on NDVI can be used as a simpler water surface detection where advanced algorithms are not available or preferred, although smaller extent of the surface is going to be identified. Following is a detail of comparison, a yellow layer of pixels with NDVI values up to -0.70 is placed on top of a red layer of pixels from the *water* class.

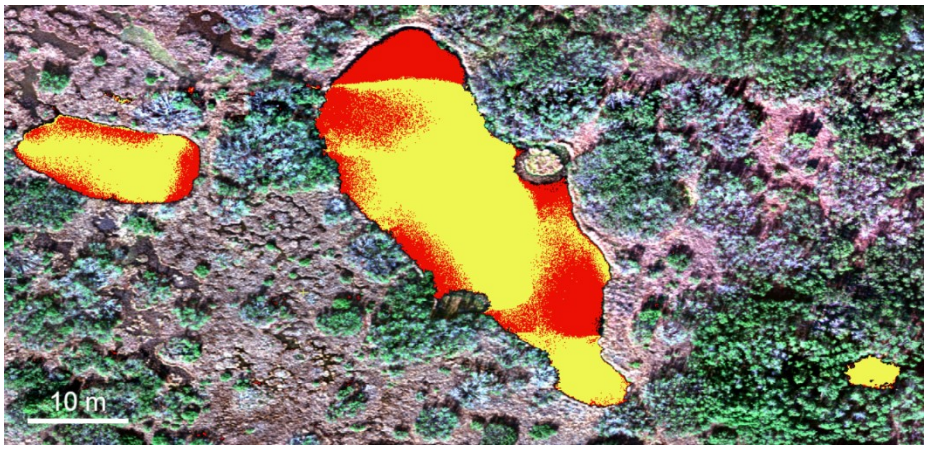

Figure 14: Water surface from NDVI values

Up to NDVI value of -0.57 there is a higher chance that the given pixel belongs to the class water than to any other category. Up to NDVI value of -0.7, it is almost certain that the pixel would be classified as water by this supervised classification.

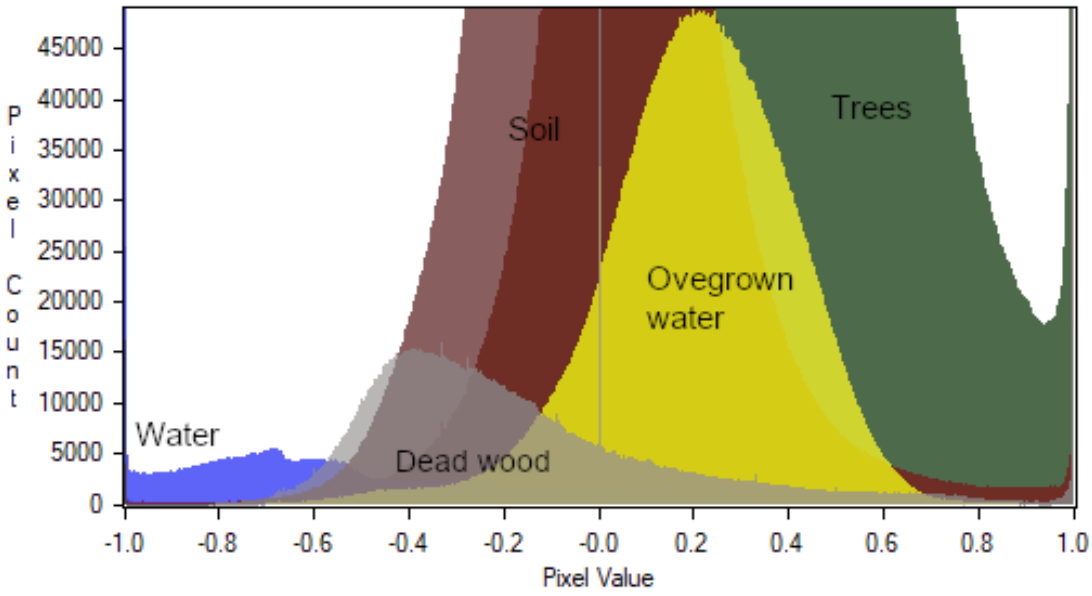

Figure 15: All classes compared NDVI values

5.3 Thermal analysis

A false colour composite for qualitative analysis and a temperature map for quantitative analysis were created.

Various land cover classes differ substantially in their thermal emissions, this can be observed in a false colour composite where red channel is shown as green and blue colours and thermal channel is shown as red:

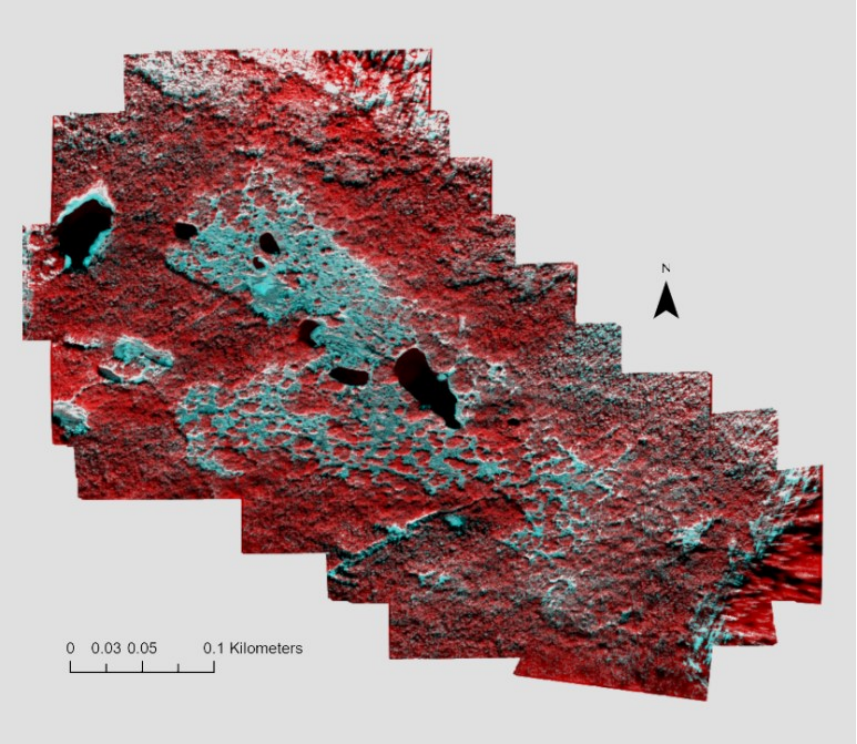

Figure 16: Thermal channel colour composite

Considering the low spatial resolution of thermal data, they can be combined with higher resolution channel for more details on the position of higher thermal emissions. A clear difference in behaviour of water surface and vegetation is observed. While water thermal emissions are very low and water shows as black in the colour composite, vegetation emits high thermal emissions.

Using the thermal channel, a map of the surface temperature was generated as well. The MicaSense Altum-PT sensor records the temperature in centikelvins, a conversion into degrees Celsius was needed. The minimum surface temperature in the study area is -3°C and maximum 22.2°C. The mean temperature is 8.9°C, median temperature is 9.1°C and the standard deviation is 2.3°C, distribution of temperature can be seen in Figure 18.

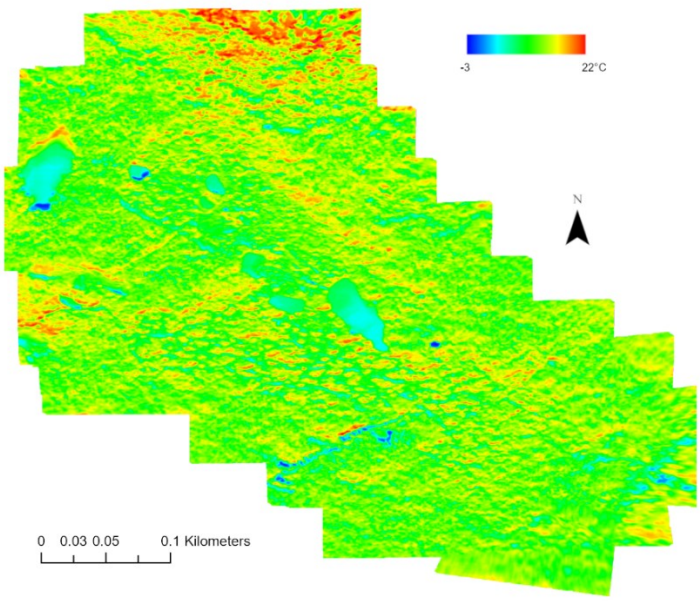

Figure 17: Temperature map

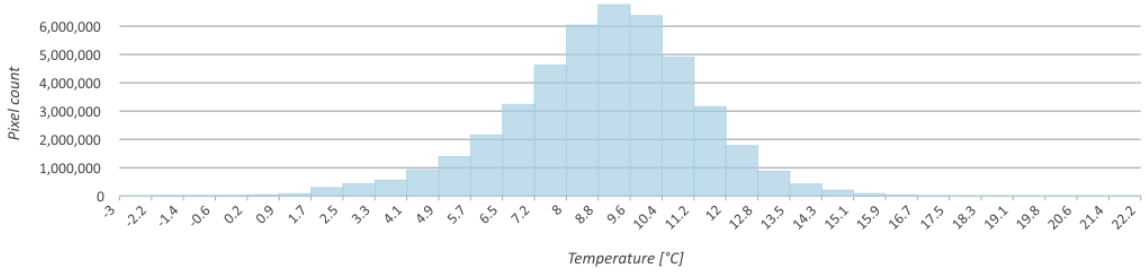

Figure 18: Temperature distribution

5.4 Digital elevation model

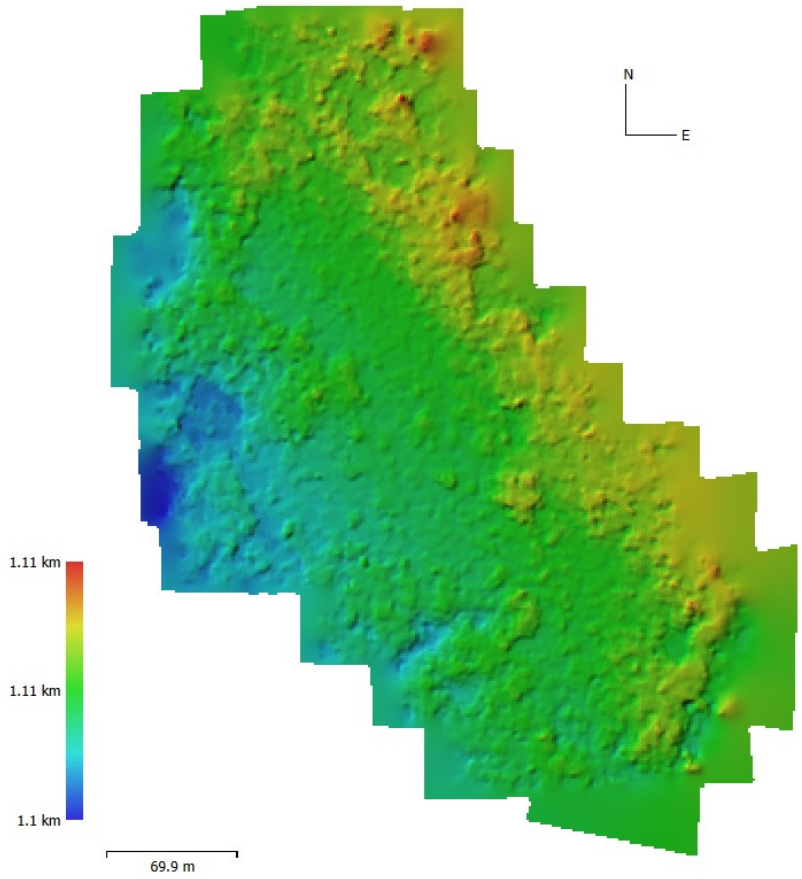

Figure 19: DEM

DEM shows little variability in height, the higher elevation in north-east is caused mostly by trees, but lower elevation towards the south-west can be observed even in areas covered by trees. A substantially lower altitude compared to the immediate surroundings can be seen in the drain, which is being revitalised in the south-western part of the map.

6. Discussion

The proposed methods of analysis of spectral data shown as an example on Rokytka peatbog combine various variables important to determine the state of a particular peatbog or its parts but rely on landcover analysis, spatial indices, and simple methods like false colour composites. A better classification of the state of the environment, like health of the vegetation, relative soil moisture or a 3D model, would be certainly helpful. Unfortunately, information on a reference group of peatbogs or quantitative data on how the ideal healthy peatbog environment looks like are not available, combined with the inability of change detection while having data from only one date, there was no possibility of comparison, and the interpretation of data is naturally lacking.

The original plan was to carry out the classification in Google Earth Engine, which is a cloud computing platform. Trial classification on a subset of data was performed with an adapted code in JavaScript by Bennett et al. (2020) but it was found that while the advantage of this platform is that the processes can truly be completely modified to suit the needs of the particular data processing needs this also causes the process to require a more advanced understanding of the partial processes. Instead, the software Catalyst Professional (former Geomatica) was used and its predefined classification workflow was utilized. The “salt-and-pepper” effect is very much present in the classification and could be eliminated by using object-based image-analysis method instead of a pixel-based one but on the detailed UAV data which have high inter-pixel variability false objects could be identified. Having access to data acquired on two or more different occasions, this kind of a simple classification could give a basic idea of temporal changes of land cover in the area.

Concerning additional ways to analyse and interpret data, some more methods of qualitative nature, which were outlined but not elaborated further, are as follows. Details of true colour composite (left) and false colour composite (near-infrared channel is shown as green, red and blue are true colour) where the overgrown ponds are visible:

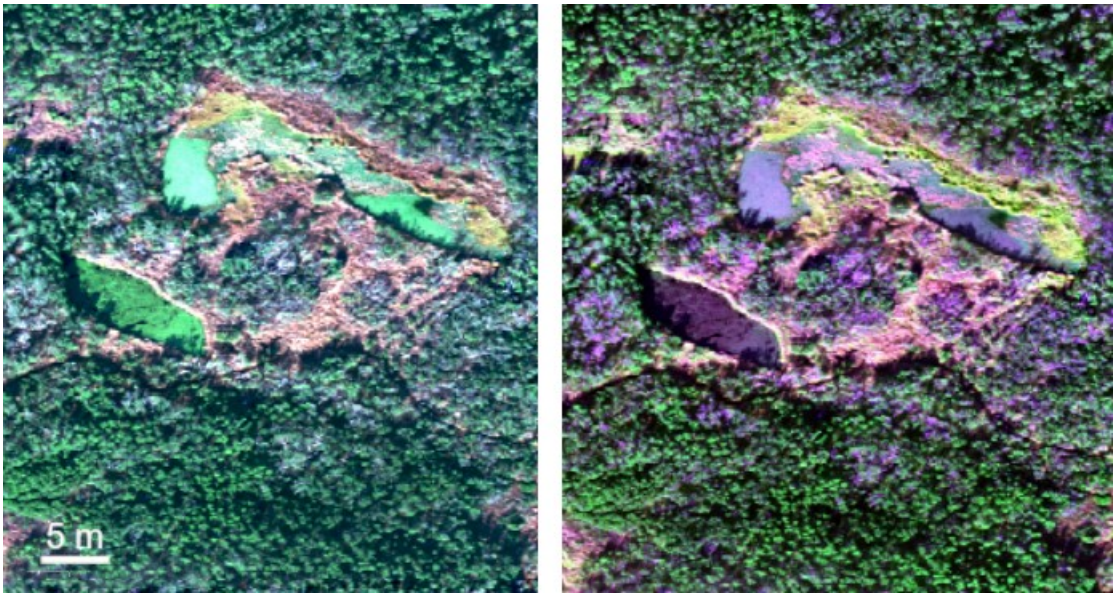

Figure 20: Overgrown ponds

The ponds have a similar spectral manifestation as trees in true colour composite and a visibly different one in this false colour composite. It could also be assessed, for example, whether it is in fact algae or whether it is cyanobacteria based on various spectral manifestations (e.g., Pu et al. 2022).

Detail of unsupervised classification on water class:

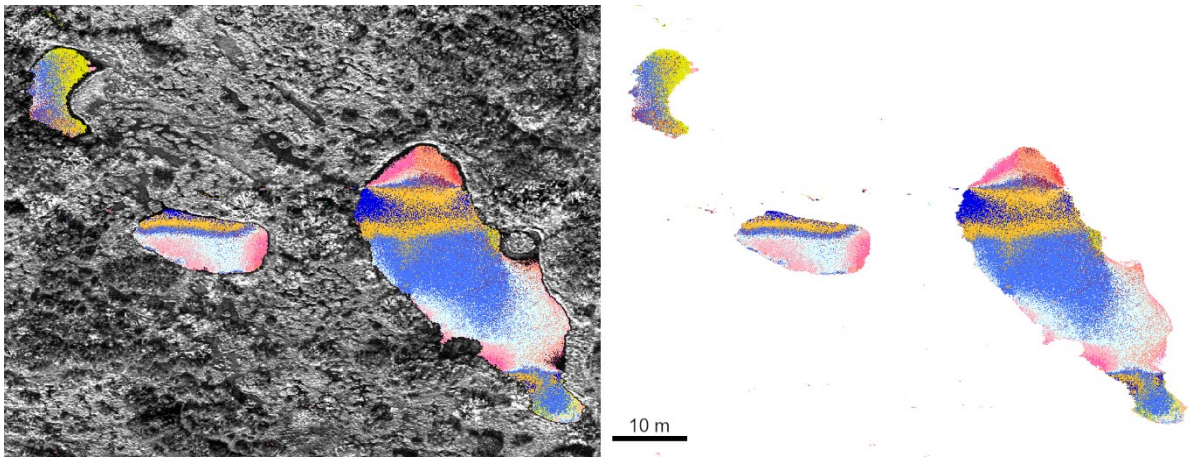

Figure 21: Water surface unsupervised classification

Different spatial manifestations of water are separated into classes, it can be further studied whether that is based on the water quality, water depth, etc. This unsupervised classification was carried out on the *water* class from supervised classification using the K-means algorithm with the default settings (Fig. 22) in Catalyst Professional.

K-Means parameters:

Parameter	Value
Max Class	16
Max Iteration	16
Min Threshold	0.010000
Max Sample Size	262144
Background	

Figure 22: Unsupervised classification parameters

The analysis carried out at Rokytka peatbog serves as an example of methods, further temporal change, particular reason for the study area monitoring, and additional context would have to be taken into consideration when evaluating the environment. UAV monitoring of peatbogs is a very broad topic with many possibilities, nonetheless it was showed that it is possible to carry out a partial analysis of UAV gathered imagery using intuitive software with built-in analysis tools. Yao et al. (2019) even state that there is room for improvement with currently wider used UAV data analysis as the potential of such detailed spatial information is not entirely utilized.

7. Conclusion

UAVs are a suitable technology to use in the circumstances of fragile peatbog ecosystems. The technology is reliable in terms of indicating water surface, plant species, evaluating the surface structure or the temperature and moisture characteristics both in the visible spectrum and in the red edge, near-infrared and thermal spectres. There are quite a few different types of data which can be sourced from sensors attached to a drone, making the acquisition of material efficient and bringing the costs down. This type of monitoring can help with keeping track of conservation and/or restoration of these easily disturbed ecosystems which offer a wide range of ecosystem services. A classification and the use of additional methods was shown on data from the Rokytka peatbog. Based on a supervised classification the vegetation structure was revealed, differences between classes were shown on NDVI values and a threshold for water surface detection was suggested. Thermal distribution was calculated, DEM was generated, and other partial analyses were outlined.

References

AIR NAVIGATION SERVICES OF THE CZECH REPUBLIC, no date. AisView 3.8. Online. [Accessed 24 April 2022]. Retrieved from: https://dronview.rlp.cz/

AMARASINGAM, Narmilan, ASHAN SALGADOE, Arachchige Surantha, POWELL, Kevin, GONZALEZ, Luis Felipe and NATARAJAN, Sijesh, 2022. *A review of UAV platforms, sensors, and applications for monitoring of sugarcane crops*. 1 April 2022. Elsevier B.V.

ARNOLD, Thomas, DE BIASIO, Martin, FRITZ, Andreas and LEITNER, Raimund, 2013. UAV-based measurement of vegetation indices for environmental monitoring. In: *Proceedings of the International Conference on Sensing Technology, ICST*. 2013. pp. 704–707. ISBN 9781467352215. DOI 10.1109/ICSensT.2013.6727744.

BENNETT, Mary K., YOUNES, Nicolas and JOYCE, Karen, 2020. Automating drone image processing to map coral reef substrates using google earth engine. *Drones*. 1 September 2020. Vol. 4, no. 3, pp. 1–13. DOI 10.3390/drones4030050.

BETTINGER, Pete, BOSTON, Kevin, SIRY, Jacek P. and GREBNER, Donald L., 2017. Geographic Information and Land Classification in Support of Forest Planning. In: *Forest Management and Planning*. Elsevier. pp. 65–85.

BEYER, Florian, JURASINSKI, Gerald, COUWENBERG, John and GRENZDÖRFFER, Görres, 2019. Multisensor data to derive peatland vegetation communities using a fixed-wing unmanned aerial vehicle. *International Journal of Remote Sensing*. 2019. Vol. 40, no. 24, pp. 9103–9125. DOI 10.1080/01431161.2019.1580825.

BLYENBURGH, 2021. RPAS Yearbooks. Online. 2021. [Accessed 21 November 2022]. Retrieved from: https://rpas-regulations.com/community-info/rpas-yearbooks/

BLYENBURGH, 2022. *The UAS Ecosystem*. Paris.

BOON, M. A., DRIJFHOUT, A. P. and TESFAMICHAEL, S., 2017. Comparison of a fixed-wing and multi-rotor UAV for environmental mapping applications: A case study. *International Archives of the Photogrammetry, Remote Sensing and Spatial Information Sciences - ISPRS Archives*. Online. 23 August 2017. Vol. 42, no. 2W6, pp. 47–54. [Accessed 4 December 2022]. DOI 10.5194/ISPRS-ARCHIVES-XLII-2-W6-47-2017.

BUFKOVÁ, Ivana, KŘENOVÁ, Zdenka and BASTL, Marek, 2021. *Ten years of changes in hydrology and vegetation in montane mires of temperate zone in Central Europe (Šumava National Park)*.

CAMBRIDGE ENGLISH DICTIONARY, no date. UAV | meaning in the Cambridge English Dictionary. Online. [Accessed 12 June 2022]. Retrieved from: https://dictionary.cambridge.org/dictionary/english/uav

CATALYST, no date. Object Analyst Classification – CATALYST.Earth. Online. [Accessed 3 July 2022]. Retrieved from: https://catalyst.earth/2021/12/01/object-analyst/#11-eael-table-of-content

CIVIL AVIATION AUTHORITY CZECH REPUBLIC, 2020. *Public Decree, General Measure*. Online. 2020. Prague. [Accessed 24 April 2022]. Retrieved from: https://www.caa.cz/wp-content/uploads/2020/11/20201230162623731.pdf?cb=df1bf0a70f0d917a9de413d0f32845bd

CLUTTERBUCK, B., CHICO, G., LABADZ, J. and MIDGLEY, N., 2018. The potential of geospatial technology for monitoring peatland environments. In: FERNÁNDEZ-GARCÍA, J.M. and PÉREZ, K.J. (eds.), *Inventory, value and restoration of peatlands and mires: recent contributions*. Bilbao: Provincial Council of Bizkaia. pp. 167–181.

COLOMINA, I. and MOLINA, P., 2014. *Unmanned aerial systems for photogrammetry and remote sensing: A review*. 1 June 2014. Elsevier B.V.

ČÚZK, no date. Geoprohlížeč, DMR 5G. Online. [Accessed 13 November 2022]. Retrieved from: https://ags.cuzk.cz/geoprohlizec/

DOLEŽAL, Tomaš, VLČEK, Lukaš, KOCUM, Jan and JANSKY, Bohumir, 2017. *Evaluation of the influence of mountain peat bogs restoration measures on the groundwater level: Case study rokytka peat bog, the šumava mts., Czech Republic*. 20 December 2017. Karolinum - Nakladatelstvi Univerzity Karlovy.

ELVIDGE, Christopher D. and CHEN, Zhikang, 1995. Comparison of broad-band and narrow-band red and near-infrared vegetation indices. *Remote Sensing of Environment*. 1 October 1995. Vol. 54, no. 1, pp. 38–48. DOI 10.1016/0034-4257(95)00132-K.

FURUKAWA, Yasutaka and HERNÁNDEZ, Carlos, 2015. Multi-View Stereo: A Tutorial. *Foundations and Trends® in Computer Graphics and Vision*. Online. 24 June 2015. Vol. 9, no. 1–2, pp. 1–148. [Accessed 6 December 2022]. DOI 10.1561/0600000052.

GONÇALVES, Gil, GONÇALVES, Diogo, GÓMEZ-GUTIÉRREZ, Álvaro, ANDRIOLO, Umberto and PÉREZ-ALVÁREZ, Juan Antonio, 2021. 3D Reconstruction of Coastal Cliffs from Fixed-Wing and Multi-Rotor UAS: Impact of SfM-MVS Processing Parameters, Image Redundancy and Acquisition Geometry. *Remote Sensing 2021, Vol. 13, Page 1222*. Online. 23 March 2021. Vol. 13, no. 6, pp. 1222. [Accessed 4 December 2022]. DOI 10.3390/RS13061222.

HORSWELL, J., 2013. Recording. In: *Encyclopedia of Forensic Sciences: Second Edition*. Elsevier Inc. pp. 368–371. ISBN 9780123821652.

IGLHAUT, Jakob, CABO, Carlos, PULITI, Stefano, PIERMATTEI, Livia, O'CONNOR, James and ROSETTE, Jacqueline, 2019. *Structure from Motion Photogrammetry in Forestry: a Review*. 15 September 2019. Springer International Publishing.

JASSEY, Vincent E. J. and SIGNARBIEUX, Constant, 2019. Effects of climate warming on *Sphagnum* photosynthesis in peatlands depend on peat moisture and species-specific anatomical traits. *Global Change Biology*. 9 November 2019. Vol. 25, no. 11, pp. 3859–3870. DOI 10.1111/gcb.14788.

KALACSKA, Margaret, ARROYO-MORA, J. Pablo, DE GEA, Julie, SNIRER, Eva, HERZOG, Carrie and MOORE, Tim R., 2013. Videographic analysis of Eriophorum vaginatum spatial coverage in an Ombotrophic bog. *Remote Sensing*. December 2013. Vol. 5, no. 12, pp. 6501–6512. DOI 10.3390/rs5126501.

KATTENBORN, Teja, EICHEL, Jana, WISER, Susan, BURROWS, Larry, FASSNACHT, Fabian E. and SCHMIDTLEIN, Sebastian, 2020. Convolutional Neural Networks accurately predict cover fractions of plant species and communities in Unmanned Aerial Vehicle imagery. *Remote Sensing in Ecology and Conservation*. 1 December 2020. Vol. 6, no. 4, pp. 472–486. DOI 10.1002/rse2.146.

KATTENBORN, Teja, LEITLOFF, Jens, SCHIEFER, Felix and HINZ, Stefan, 2021. *Review on Convolutional Neural Networks (CNN) in vegetation remote sensing*. . 1 March 2021. Elsevier B.V.

KNOTH, Christian, KLEIN, Birte, PRINZ, Torsten and KLEINEBECKER, Till, 2013. Unmanned aerial vehicles as innovative remote sensing platforms for high-resolution infrared imagery to support restoration monitoring in cut-over bogs. GOSLEE, Sarah (ed.), *Applied Vegetation Science*. Online. 1 July 2013. Vol. 16, no. 3, pp. 509–517. [Accessed 5 July 2022]. DOI 10.1111/avsc.12024.

LEHMANN, Jan, MÜNCHBERGER, Wiebke, KNOTH, Christian, BLODAU, Christian, NIEBERDING, Felix, PRINZ, Torsten, PANCOTTO, Verónica and KLEINEBECKER, Till, 2016. High-Resolution Classification of South Patagonian Peat Bog Microforms Reveals Potential Gaps in Up-Scaled CH4 Fluxes by use of Unmanned Aerial System (UAS) and CIR Imagery. *Remote Sensing*. Online. 25 February 2016. Vol. 8, no. 3, pp. 173. [Accessed 2 November 2022]. DOI 10.3390/rs8030173.

LEHMANN, Jan R.K., PRINZ, Torsten, ZILLER, Silvia R., THIELE, Jan, HERINGER, Gustavo, MEIRA-NETO, João A.A. and BUTTSCHARDT, Tillmann K., 2017. Open-source processing and analysis of aerial imagery acquired with a low-cost Unmanned Aerial System to support invasive plant management. *Frontiers in Environmental Science*. 11 July 2017. Vol. 5, no. JUL. DOI 10.3389/fenvs.2017.00044.

LENDZIOCH, Theodora, LANGHAMMER, Jakub, VLČEK, Lukáš and MINAŘÍK, Robert, 2021. Mapping the groundwater level and soil moisture of a montane peat bog using uav monitoring and machine learning. *Remote Sensing*. 1 March 2021. Vol. 13, no. 5, pp. 1–30. DOI 10.3390/rs13050907.

LIFE FOR MIRES, no date. LIFE for MIRES – život pro mokřady. Online. [Accessed 11 June 2022]. Retrieved from: https://life.npsumava.cz/

LUSCOMBE, David J., ANDERSON, Karen, GATIS, Naomi, GRAND-CLEMENT, Emilie and BRAZIER, Richard E., 2015. Using airborne thermal imaging data to measure near-surface hydrology in upland ecosystems. *Hydrological Processes*. 15 March 2015. Vol. 29, no. 6, pp. 1656–1668. DOI 10.1002/hyp.10285.

MICASENSE, no date. Altum-PT - MicaSense. Online. [Accessed 11 June 2022]. Retrieved from: https://micasense.com/altum-pt/

MICHELETTI, Natan, CHANDLER, Jim H and LANE, Stuart N, 2015. Structure from Motion (SfM) Photogrammetry. *British Society for Geomorphology Geomorphological Techniques*. 2015. Vol. 2, no. 2, pp. 1–12. DOI 10.5194/isprsarchives-XL-5-W4-37-2015.

MUSA, Z. N., POPESCU, I. and MYNETT, A., 2015. *A review of applications of satellite SAR, optical, altimetry and DEM data for surface water modelling, mapping and parameter estimation*. 1 September 2015. Copernicus GmbH.

NEX, F., ARMENAKIS, C., CRAMER, M., CUCCI, D. A., GERKE, M., HONKAVAARA, E., KUKKO, A., PERSELLO, C. and SKALOUD, J., 2022. *UAV in the advent of the twenties: Where we stand and what is next*. 1 February 2022. Elsevier B.V.

NEX, Francesco and REMONDINO, Fabio, 2014. UAV for 3D mapping applications: A review. *Applied Geomatics*. Online. 8 November 2014. Vol. 6, no. 1, pp. 1–15. [Accessed 5 December 2022]. DOI 10.1007/S12518-013-0120-X/FIGURES/11.

PU, Jing, SONG, Kaishan, LV, Yunfeng, LIU, Ge, FANG, Chong, HOU, Junbin and WEN, Zhidan, 2022. Distinguishing Algal Blooms from Aquatic Vegetation in Chinese Lakes Using Sentinel 2 Image. *Remote Sensing*. Online. 21 April 2022. Vol. 14, no. 9, pp. 1988. [Accessed 9 July 2022]. DOI 10.3390/rs14091988.

RADOGLOU-GRAMMATIKIS, Panagiotis, SARIGIANNIDIS, Panagiotis, LAGKAS, Thomas and MOSCHOLIOS, Ioannis, 2020. A compilation of UAV applications for precision agriculture. *Computer Networks*. 8 May 2020. Vol. 172. DOI 10.1016/j.comnet.2020.107148.

RAEVA, Paulina Lyubenova, ŠEDINA, Jaroslav and DLESK, Adam, 2019. Monitoring of crop fields using multispectral and thermal imagery from UAV. *European Journal of Remote Sensing*. Online. 28 March 2019. Vol. 52, no. sup1, pp. 192–201. [Accessed 11 June 2022]. DOI 10.1080/22797254.2018.1527661.

RAI, Ved Prakash, RANJAN, Rajeev, GADHIYA, Ankit R. and MOTE, Balaji M., 2021. Use of modern physical tools for mitigating the effect of abiotic stresses. In: *Stress Tolerance in Horticultural Crops*. Elsevier. pp. 387–397. ISBN 9780128228494.

REISCHIG, Thomas and CORDES, Hiltrud, 2020. Drones for Turtles. In: *Sea Turtle Research and Conservation: Lessons From Working In The Field*. Elsevier. pp. 57–67. ISBN 9780128210291.

SCHONBERGER, Johannes L. and FRAHM, Jan Michael, 2016. Structure-from-Motion Revisited. *Proceedings of the IEEE Computer Society Conference on Computer Vision*

and Pattern Recognition. Online. 9 December 2016. Vol. 2016-December, pp. 4104–4113. [Accessed 4 December 2022]. DOI 10.1109/CVPR.2016.445.

SEIER, Gernot, HÖDL, Claudia, ABERMANN, Jakob, SCHÖTTL, Stefan, MARINGER, Alexander, HOFSTADLER, Daniel N., PRÖBSTL-HAIDER, Ulrike and LIEB, Gerhard K., 2021. *Unmanned aircraft systems for protected areas: Gadgetry or necessity?*. 1 December 2021. Elsevier GmbH.

TYMKÓW, Przemysław, JÓŹKÓW, Grzegorz, WALICKA, Agata, KARPINA, Mateusz and BORKOWSKI, Andrzej, 2019. Identification of water body extent based on remote sensing data collected with unmanned aerial vehicle. *Water (Switzerland)*. 16 February 2019. Vol. 11, no. 2. DOI 10.3390/w11020338.

UKHUREBOR, Kingsley Eghonghon, ADETUNJI, Charles Oluwaseun, OLUGBEMI, Olaniyan T., NWANKWO, W., OLAYINKA, Akinola Samson, UMEZURUIKE, C. and HEFFT, Daniel Ingo, 2022. Precision agriculture: Weather forecasting for future farming. In: *AI, Edge and IoT-based Smart Agriculture*. Elsevier. pp. 101–121.

VLČEK, Lukáš, KOCUM, Jan, JANSKÝ, Bohumír, ŠEFRNA, Luděk and KUČEROVÁ, Andrea, 2012. Retention potential and hydrological balance of a peat bog: case study of Rokytka Moors, Otava River headwaters, sw. Czechia. *Geografie*. 2012. Vol. 117, no. 4, pp. 395–414. DOI 10.37040/geografie2012117040395.

WOELLNER, Romy and WAGNER, Thomas C., 2019. Saving species, time and money: Application of unmanned aerial vehicles (UAVs) for monitoring of an endangered alpine river specialist in a small nature reserve. *Biological Conservation*. 1 May 2019. Vol. 233, pp. 162–175. DOI 10.1016/j.biocon.2019.02.037.

YAO, Huang, QIN, Rongjun and CHEN, Xiaoyu, 2019. Unmanned Aerial Vehicle for Remote Sensing Applications—A Review. *Remote Sensing*. Online. 18 June 2019. Vol. 11, no. 12, pp. 1443. [Accessed 16 May 2022]. DOI 10.3390/rs11121443.

ZHANG, Ce, ATKINSON, Peter M., GEORGE, Charles, WEN, Zhaofei, DIAZGRANADOS, Mauricio and GERARD, France, 2020. Identifying and mapping individual plants in a highly diverse high-elevation ecosystem using UAV imagery and deep learning. *ISPRS Journal of Photogrammetry and Remote Sensing*. 1 November 2020. Vol. 169, pp. 280–291. DOI 10.1016/j.isprsjprs.2020.09.025.

List of figures

List of tables

Appendix

Attached in digital version are the study area orthomosaic and classification.